Advances in Science and Technology Research Journal

Advances in Science and Technology Research Journal, 2025, 19(8), 285–295
https://doi.org/10.12913/22998624/205744
ISSN 2299-8624, License CC-BY 4.0

Received: 2025.01.29
Accepted: 2025.06.15
Published: 2025.07.01

Performance analysis of tantalum and copper patches in micro-electro-mechanical systems based microstrip patch antennas for 5th generation mmWave applications

Redia Mohd Redzuwan[1*], Jahariah Sampe[1], Rhonira Latif[1], Zeti Akma Rhazali[2], Noor Hidayah Mohd Yunus[3]

[1] Institute of Microengineering and Nanoelectronics, Universiti Kebangsaan Malaysia, Bangi, Selangor, Malaysia
[2] Institute of Energy Infrastructure (IEI), Universiti Tenaga Nasional, Kajang, Selangor, Malaysia
[3] Advanced Telecommunication Technology, Communication Technology Section, Universiti Kuala Lumpur British Malaysian Institute, Selangor, Malaysia
* Corresponding author's e-mail: redia@uniten.edu.my

ABSTRACT

The rapid advancement of 5th generation (5G) technology has driven the demand for high performance millimetre-wave (mmWave) antennas with enhanced efficiency and scalability. However, designing microstrip patch antennas (MPAs) at mmWave frequencies presents challenges in optimizing gain, bandwidth, and voltage standing wave ratio (VSWR) while maintaining cost-effectiveness and fabrication feasibility. This study proposes a novel MPA design incorporating an ET-shaped slot and three parasitic rectangular patches to achieve a balance between gain, bandwidth, and VSWR. The micro-electro-mechanical systems (MEMS) based design explores tantalum and copper as alternative patch materials for 28 GHz radio frequency (RF) energy harvesting in 5G mmWave systems. CST simulations are conducted to evaluate key performance metrics, including VSWR, gain, and reflection coefficient, S_{11} across material thicknesses of 35 µm, 1 µm, and 700 nm. Among the tested configurations, the 1 µm thick tantalum patch demonstrates the best performance, achieving an S_{11} of -21.474 dB, a VSWR of 1.18, and a gain of 6.14 dB at 28 GHz. These findings highlight tantalum's potential as a scalable, high-performance material for MEMS-based 5G mmWave antenna applications.

Keywords: microstrip patch antenna, MEMS; millimetre-wave applications, tantalum and copper patch, 5G applications.

INTRODUCTION

The fifth generation (5G) of wireless communication networks represents a major advancement in mobile technology, surpassing the capabilities of previous generations like 3G and 4G. It offers faster speeds, lower latency, higher capacity, and broader bandwidth [1]. A key advantage of 5G is its significantly higher data transfer rates compared to 4G, enabling efficient media streaming and faster downloads [2]. The reduced latency characteristic of 5G networks is crucial for applications requiring real-time data transmission, including augmented reality (AR) and virtual reality (VR). Moreover, 5G networks can support a significantly greater number of connected devices, which is particularly important in densely populated areas with high connectivity demands. This enhanced connectivity opens new avenues for expanding energy sources and optimizing energy harvesting technologies [3].

Energy harvesting typically involves small systems that generate small amounts of power [4]. Among the most common sources of small-scale energy are environmental mechanical energy [5], body heat, and radio frequency (RF) energy [6]. Innovative designs, such as energy harvesters that integrate magnetic springs within

electromagnetic vibration generators, have been developed to optimize the conversion of mechanical vibrations into electrical energy [7]. Additionally, environmental factors, such as air pollution, can influence the intensity of received signals in wireless communication systems, potentially affecting the efficiency of RF energy harvesting in 5G networks [8]. Given these environmental interactions, micro-energy harvesting from ambient RF sources presents a promising opportunity, particularly in urban areas where radio and television broadcasts, mobile phone services, and wireless local area networks (WLANs) are pervasive. Micro-scale energy harvesting systems, such as rectennas and piezoelectric transducers, typically produce very low power outputs, often in the range of a few milliwatts [9]. This poses a significant challenge in designing these systems, as the generated power may be insufficient to operate devices with higher energy demands [10].

To address the limitations of low power output in micro-energy harvesting systems, developing high-performance antennas is essential for capturing more environmental energy and improving overall system efficiency. Microstrip patch antennas (MPAs) emerge as an ideal solution for systems operating at 5G network frequencies, offering benefits such as compact size, lightweight design, cost-effectiveness, and ease of construction [11]. Figure 1 illustrates the fundamental design of the microstrip patch antenna, featuring a metal patch elevated above the ground plane, with a thin dielectric layer acting as the separator. The patch and ground, typically made of copper or gold, can be fabricated in a variety of shapes including rectangular, circular, triangular, or annular ring designs.

Optimizing the performance of MPAs for millimeter-wave (mmWave) applications requires the careful selection of materials for both the patch and ground plane [12]. The material must possess high electrical conductivity to minimize resistive losses and ensure efficient signal transmission

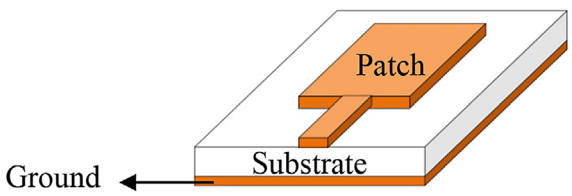

Figure 1. Fundamental design of a rectangular microstrip patch antenna

[13]. Equally important is thermal stability, as high-frequency operations generate significant heat, necessitating materials that can withstand elevated temperatures without degradation. Mechanical strength and durability are crucial to prevent deformation during fabrication and operation, especially when employing advanced techniques like micro-electro-mechanical systems (MEMS) [14]. Additionally, corrosion resistance is vital for maintaining the antenna's long-term reliability in diverse environmental conditions.

While copper remains the most widely used patch material due to its superior electrical conductivity and affordability, researchers have explored alternative materials such as aluminium, gold, silver, and tantalum to improve performance. Aluminium offers a lightweight alternative but has slightly lower conductivity, making it ideal for flexible and wearable MPAs. Gold provides excellent conductivity and oxidation resistance, making it suitable for high-performance applications, though its high cost is a limiting factor. Silver, the most conductive metal, is less commonly used due to tarnishing and cost constraints. Despite growing interest in alternative materials, tantalum remains underexplored in MPA design. To address these gaps, this research introduces the following novel contributions:

- comparative performance analysis of tantalum and copper: this research investigates tantalum as an alternative patch material in MEMS-based MPAs for 5G mmWave applications and evaluates tantalum's suitability and efficiency compared to copper, which remains a widely used choice in antenna applications;
- comprehensive performance evaluation: the study employs CST software to analyze key performance parameters, including VSWR, gain, reflection coefficient, S_{11}, and bandwidth, providing detailed insights into tantalum's capabilities;
- investigation of patch height influence: this study explores the impact of patch height on antenna efficiency, an aspect that remains underexplored in tantalum-based MPAs;
- novel MPA design incorporating an ET-shaped slot and three parasitic rectangular patches: this research presents an innovative MPA configuration featuring an ET-shaped slot and three parasitic rectangular patches, enhancing impedance matching, bandwidth, and overall antenna performance for 5G mmWave applications.

- guidance for future MEMS-based MPA designs: by providing insights into the feasibility of tantalum for 5G mmWave applications, this study helps advance the development of next-generation high-performance and durable MPAs.

RESEARH BACKGROUND

In microstrip patch antenna design, the selection of patch material plays a vital role in determining overall performance. Copper has traditionally been the preferred material because of its superior electrical conductivity and affordability, making it an ideal choice for various applications [15]. Authors in [16] present a novel design of a dual band MPA that operates at 28 GHz and 46 GHz frequencies, which are crucial for the development of 5G communication systems. The authors designed a rectangular microstrip patch antenna with two rectangular slots (semicircular at both ends) on the patch, using a copper patch and ground plate. At 28 GHz, the antenna achieves a return loss of -45.21 dB and a bandwidth of 1.84 GHz, while at 46 GHz, the reflection coefficient, S_11 is -39.60 dB, and the bandwidth is 9.00 GHz. Additionally, the voltage standing wave ratio (VSWR) values are 1.011 and 1.021 at 28 GHz and 46 GHz, respectively, indicating good impedance matching. However, this paper reports a lower gain at 46 GHz, which is 5.84 dB compared to 6.25 dB at 28 GHz. The design presented in this paper aligns well with the requirements of 5G communication systems, which demand higher bandwidth, lower reflection coefficient, and higher directivity to provide better connectivity and efficiency.

With the growing demand for high performance and specialized applications, especially in the mmWave band, researchers have explored alternative materials with enhanced properties. Recent studies on MPAs have investigated the use of various patch materials, including aluminum [14], gold [17], silver [18], and tantalum. Aluminum, as a lightweight alternative to copper, is particularly advantageous in applications where weight is a concern such as flexible and wearable MPAs, despite its slightly lower conductivity [14]. Gold, on the other hand, is widely employed in high-performance and space-related applications due to its superior conductivity and oxidation resistance, though its high cost limits its applicability. Silver, while boasting the highest conductivity among metals, faces challenges such as tarnishing and high expense, making it less widely used in antenna applications [19].

Previous research has demonstrated the performance of these materials. For instance, authors in [20] conducted performance analysis and simulation of rectangular-shaped MPAs with gold, copper, and silver patches for mmWave 5G applications. The study revealed that the gold patch antenna exhibited the best overall performance, achieving an S_{11} of -58.757 dB, a VSWR of 1.002, and a gain of 7.168 dB at 27.01 GHz. This superior performance is attributed to gold's higher current-carrying capacity and better conductivity compared to copper and silver. Silver, despite offering the highest bandwidth of 4.78 GHz at 26.807 GHz, suffered from tarnishing related drawbacks. Copper, on the other hand, showed a competitive gain of 7.156 dB at a resonant frequency of 26.7982 GHz, which is close to that of gold. Although gold has superior conductivity, copper is less costly, making copper a particularly suitable choice for cost-sensitive applications, such as consumer electronics.

Tantalum has shown significant promise as a patch material for specialized applications due to its durability and corrosion resistance, making it suitable for high-frequency operations like 5G mmWave bands [19]. In this study [21], tantalum's return loss performance was examined, achieving -23.525 dB, while silver exhibited the poorest performance at -17.17 dB. This study involved patch conductors, including copper, aluminum, gold, silver, iron, platinum, tantalum, and molybdenum, designed with consistent dimensions for comparison. Despite tantalum's robust performance, its operating frequency slightly deviated from the target, resonating at 27.92 GHz instead of the intended 28 GHz. Furthermore, critical performance metrics, such as gain and bandwidth, have not been reported and the influence of design parameters like patch height on antenna efficiency remains unexplored. These limitations leave gaps in understanding tantalum's full potential compared to conventional materials like copper.

PROPOSED ANTENNA DESIGN

When designing MPAs, it is critical to ensure that the design parameters align with the target frequency and application requirements. A common rule of thumb is that the height of the patch

denoted as m_t, should be significantly less than the operating wavelength, λ_0 with the recommended range being $0.03\ \lambda_0 \leq m_t \leq 0.05\ \lambda_0$. The choice of dielectric material for the substrate plays a crucial role, as its relative permittivity, ε_r significantly influences the antenna's bandwidth and gain. Low loss tangent materials are preferred to minimize electromagnetic wave absorption and energy loss, ensuring optimal performance.

In this research, a rectangular MPA is designed with a substrate height, h_s of 0.70 mm, optimized for operation at 28 GHz in mmWave 5G systems. A borosilicate glass substrate is selected for its relative permittivity, ε_r of 4.4 which offers a good balance between bandwidth and efficiency. The use of borosilicate glass also aligns with the need for robust and reliable materials in MEMS-based applications.

The antenna is designed to be fed using an inset microstrip line, a feeding technique that is known for its efficiency in achieving good impedance matching between the antenna and the transmission line. The 50 Ω impedance is a widely adopted standard in microwave and RF system design, as it provides a good balance between power-handling capability, ease of interconnection with other components, and the ability to minimize reflections while maximizing power transfer. The dimensions, specifically the length and width, of the rectangular microstrip patch antenna can be calculated using the following Equation 1 until 5 [22]:

$$W_p = \frac{C}{2f_o}\sqrt{\frac{2}{\epsilon_r + 1}} \tag{1}$$

$$L_p = \frac{C}{2f_o\sqrt{\epsilon_{eff}}} - 2\left[0.412\, h_s \frac{\left(\epsilon_{eff} + 0.3\right)\left(\frac{W_p}{h_s} + 0.264\right)}{\left(\epsilon_{eff} - 0.258\right)\left(\frac{W_p}{h_s} + 0.8\right)}\right] \tag{2}$$

$$\epsilon_{eff} = \frac{\epsilon_r + 1}{2} + \frac{\epsilon_r + 1}{2}\left(1 + 12\frac{h_s}{W_p}\right)^{-1/2} \tag{3}$$

where: W_p – patch width, L_p – length of patch, f_o – resonant frequency, C – 3×10^8 ms^{-1}, speed of light, ε_r – relative permittivity, h_s – substrate thickness, ϵ_{eff} – effective dielectric constant.

For a 50 Ω impedance matched microstrip edge patch line, the inset feed length, G of the patch in Equation 4 is derived as follows:

$$50 = Z_0\left[\cos\left(\frac{\pi G}{L_p}\right)\right]^2 \tag{4}$$

where: the patch's impedance, $Z_0 Z_0$ can be defined by:

$$Z_0 = \frac{90}{\epsilon_r - 1}\left[\frac{\epsilon_r L_p}{W_p}\right]^2 \tag{5}$$

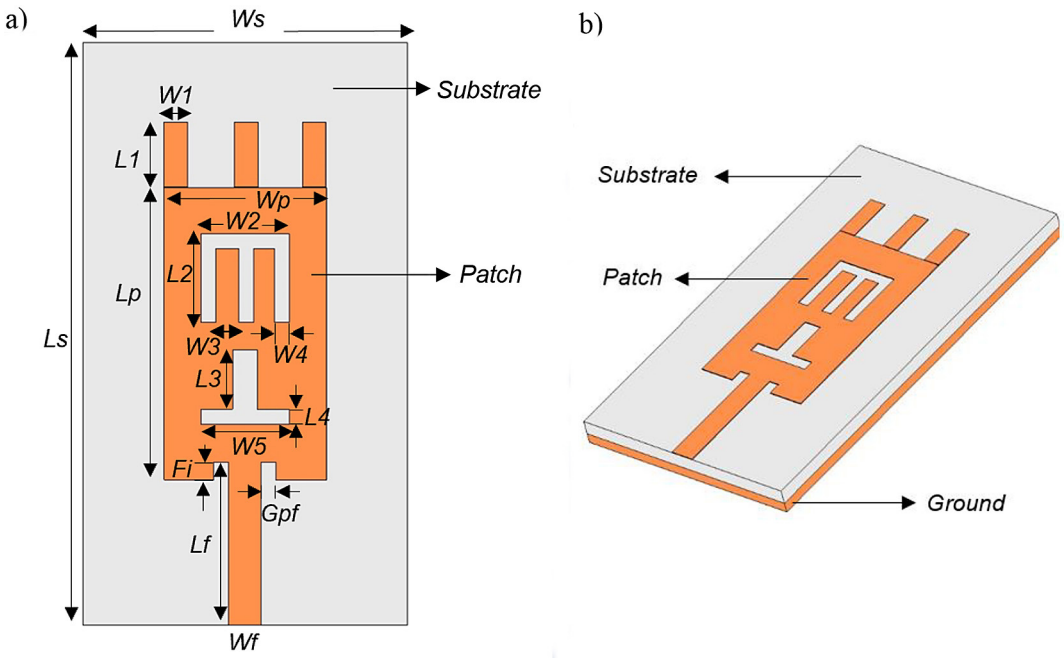

Figure 2. Geometry of the proposed microstrip patch antenna: a) top view, b) perspective view

Antenna configuration

Microstrip patch antennas were designed and simulated in CST Microwave Studio to optimize performance at 28 GHz for 5G mmWave applications. Copper and tantalum were used as patch and ground materials, with thicknesses of 35 µm, 1 µm, and 700 nm tested to explore trade-offs between fabrication feasibility and performance in MEMS-based designs. The antenna design features a rectangular patch with an ET-shaped slot and three parasitic rectangular patches to enhance radiation properties, as illustrated in Figure 2.

Detailed design parameters are provided in Table 1. All designs shared the same dimensions except for the tantalum patch at 700 nm. For this configuration, achieving the 28 GHz frequency required slight adjustments: patch width, W_p changed from 5.50 mm to 5.54 mm, and feed length, L_f from 5.52 mm to 5.54 mm.

RESULTS

Simulations for the six proposed designs were conducted using the parameter values specified in Table 1. Several antenna properties, including reflection coefficient, S_{11} bandwidth, VSWR, radiation pattern, and gain, were analysed in the 26 GHz to 29 GHz frequency range.

Reflection coefficient, S_{11} and bandwidth

Figure 3 illustrates the resonant frequencies and the reflection coefficient, S_{11} for copper and tantalum at three patch thicknesses: 35 µm, 1 µm, and 700 nm. The VSWR decreases consistently as patch thickness reduces from 35 µm to 1 µm for both copper and tantalum. The best reflection coefficient, S_{11} is observed for the copper patch at 35 µm, with a value of -27.391 dB, followed closely by tantalum at 35 µm, with -25.499 dB, representing a reduction of approximately 6.9%. The lowest reflection coefficient is seen for the tantalum patch at 700 nm, with a value of -21.145 dB.

While copper achieves a favorable S_{11} value, tantalum consistently offers a broader bandwidth. At 35 µm, tantalum achieves the widest bandwidth of 0.807 GHz, compared to 0.788 GHz for copper, a crucial advantage for efficient signal transmission in 5G applications. Data from Figure

Table 1. Design parameters of the proposed antenna

Material	Copper			Tantalum		
Patch and ground thicknesses, (m_t)	35 mm	1 µm	700 nm	35 mm	1 µm	700 nm
Antenna parameters, (mm)						
W_g	11.00	11.00	11.00	11.00	11.00	11.08
L_g	19.70	19.70	19.70	19.70	19.70	19.70
W_p	5.50	5.50	5.50	5.50	5.50	5.54
fL_p	9.85	9.85	9.85	9.85	9.85	9.85
W_s	11.00	11.00	11.00	11.00	11.00	11.08
L_s	19.70	19.70	19.70	19.70	19.70	19.70
L_f	5.52	5.52	5.52	5.52	5.52	5.54
W_f	1.11	1.11	1.11	1.11	1.11	1.11
G_{pf}	0.50	0.50	0.50	0.50	0.50	0.50
F_i	0.60	0.60	0.60	0.60	0.60	0.60
W1	0.80	0.80	0.80	0.80	0.80	0.80
L1	2.20	2.20	2.20	2.20	2.20	2.20
W2	3.00	3.00	3.00	3.00	3.00	3.00
W3	0.80	0.80	0.80	0.80	0.80	0.80
W4	0.50	0.50	0.50	0.50	0.50	0.50
L2	3.00	3.00	3.00	3.00	3.00	3.00
W5	3.00	3.00	3.00	3.00	3.00	3.00
L3	2.00	2.00	2.00	2.00	2.00	2.00
L4	0.50	0.50	0.50	0.50	0.50	0.50

3 shows tantalum maintains a wider bandwidth across all thickness variations. However, reducing thickness to 700 nm does not significantly improve bandwidth for either material. The 1 µm thickness strikes the optimal balance between minimizing S_{11} and maintaining bandwidth, making it the most suitable choice. Notably, the bandwidth narrows by only 4%, indicating minimal impact on signal performance.

Voltage standing wave ratio

The VSWR is an important factor in antenna performance, as it represents how effectively the impedance between the antenna and the transmission line or feed system is matched. In the case presented in Figure 4, the consistent VSWR values below 2 across various thicknesses of copper and tantalum indicate that the antenna operates with an efficient impedance match, minimizing power reflection and optimizing transmission performance. This stability suggests the antenna design is well-optimized to maintain a consistent impedance match across the tested thicknesses, ensuring efficient operation over a broad frequency range.

Gain and directivity

The experimental results shown in Figure 5 illustrate the simulated gain for the three copper and tantalum patch thicknesses. While the highest gain of 6.54 dB was achieved with the copper patch at 35 µm thickness, tantalum performed comparably, delivering a gain of 6.33 dB at the same thickness, reflecting only a slight decrease of 3.21%.

Even at reduced thicknesses, tantalum maintains consistent performance. The gain at 700 nm for tantalum remains within an acceptable range at 6.11 dB, corresponding to a 6.57% reduction

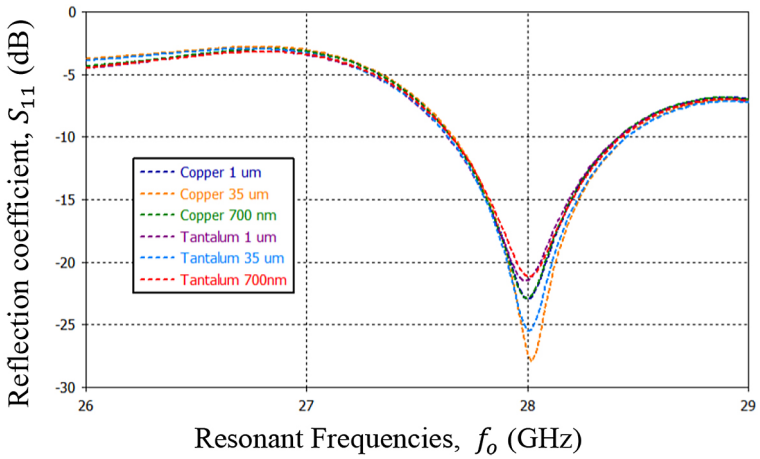

Figure 3. Resonant frequencies, f_o and reflection coefficient, S_{11} for copper and tantalum patch at various thicknesses

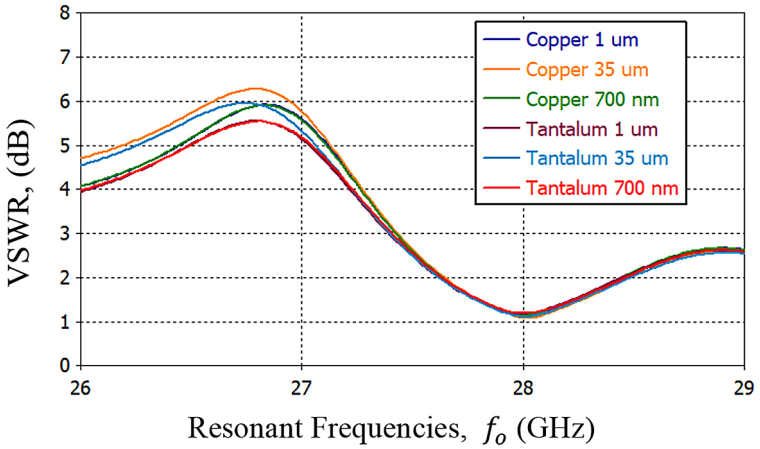

Figure 4. Voltage standing wave ratio for copper and tantalum patch at various thicknesses

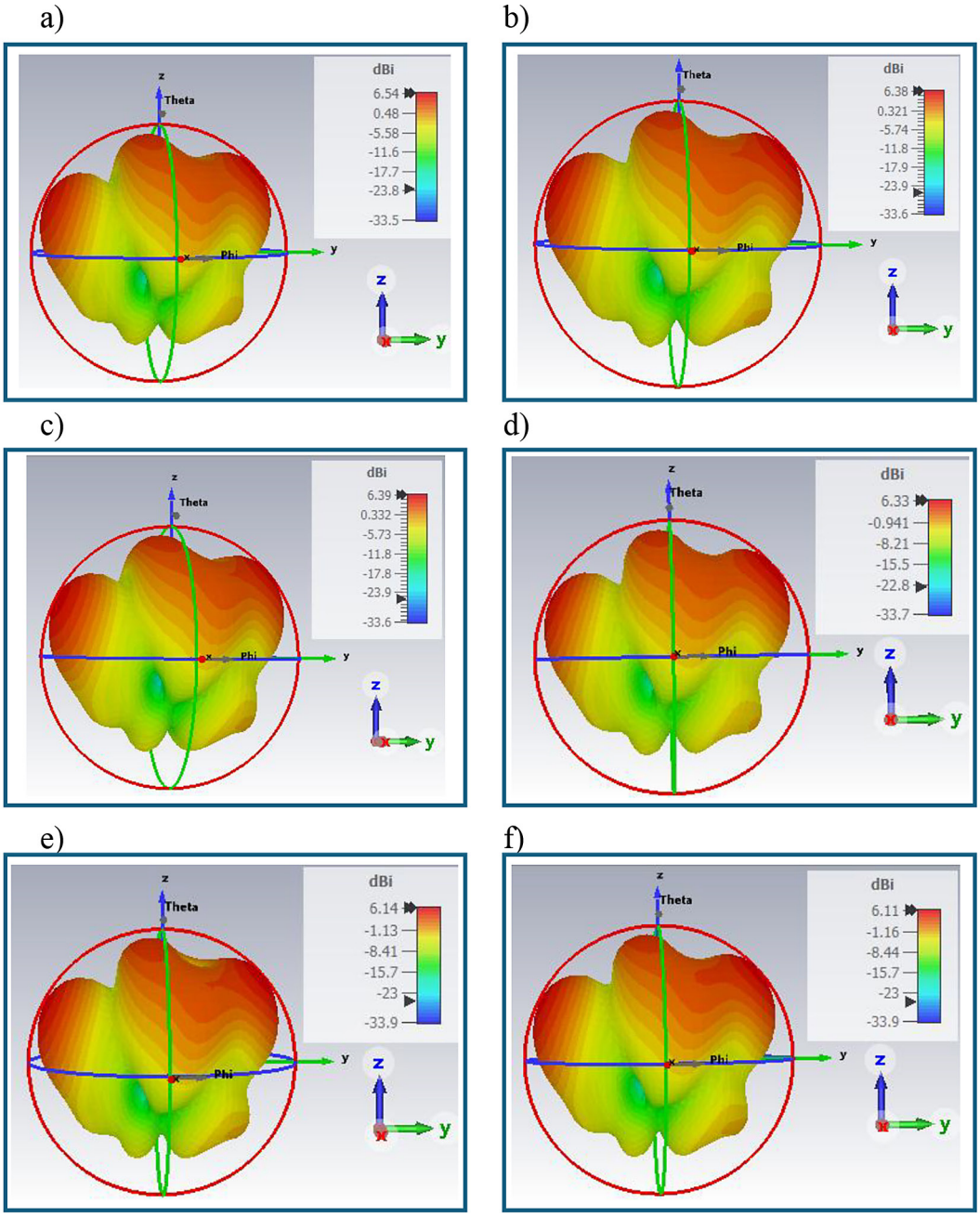

Figure 5. Simulated gain for copper and tantalum patches across different thicknesses: (a) 35 µm copper patch, (b) 1 µm copper patch, (c) 700 nm copper patch, (d) 35 µm tantalum patch, (e) 1 µm tantalum patch, (f) 700 nm tantalum patch

compared to the 35 µm copper patch. Despite this reduction, tantalum's gain values remain above 5 dB across all thicknesses, ensuring sufficient radiation efficiency for 5G applications. This highlights tantalum's suitability for thinner designs, offering a balance of gain and robustness.

Radiation pattern

The radiation patterns of the microstrip patch antenna are examined in two orthogonal planes: the E-plane and the H-plane. The E-plane corresponds to the x-z plane ($\phi = 0°$), while the H-plane corresponds to the y-z plane ($\phi = 90°$). In the far-field region, the electric field is oriented in the E-plane, whereas the magnetic field is located in the H-plane. Figure 6 and Figure 7 illustrate the radiation patterns for both planes, showcasing the performance of copper and tantalum patches at three different thicknesses. These results validate that all proposed antennas effectively produce a broadside and omnidirectional radiation pattern

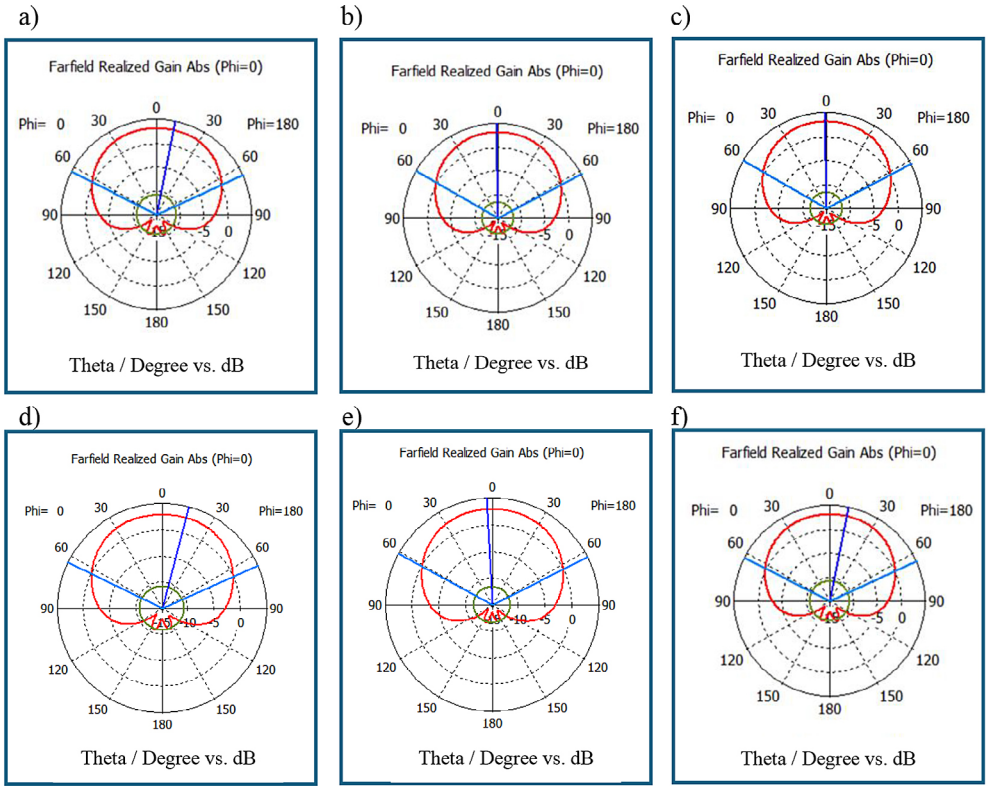

Figure 6. Radiation patterns for E (x-z) plane for copper and tantalum patch across different thicknesses: (a) 35 µm copper patch, (b) 1 µm copper patch, (c) 700 nm copper patch, (d) 35 µm tantalum patch, (e) 1 µm tantalum patch, (f) 700 nm tantalum patch

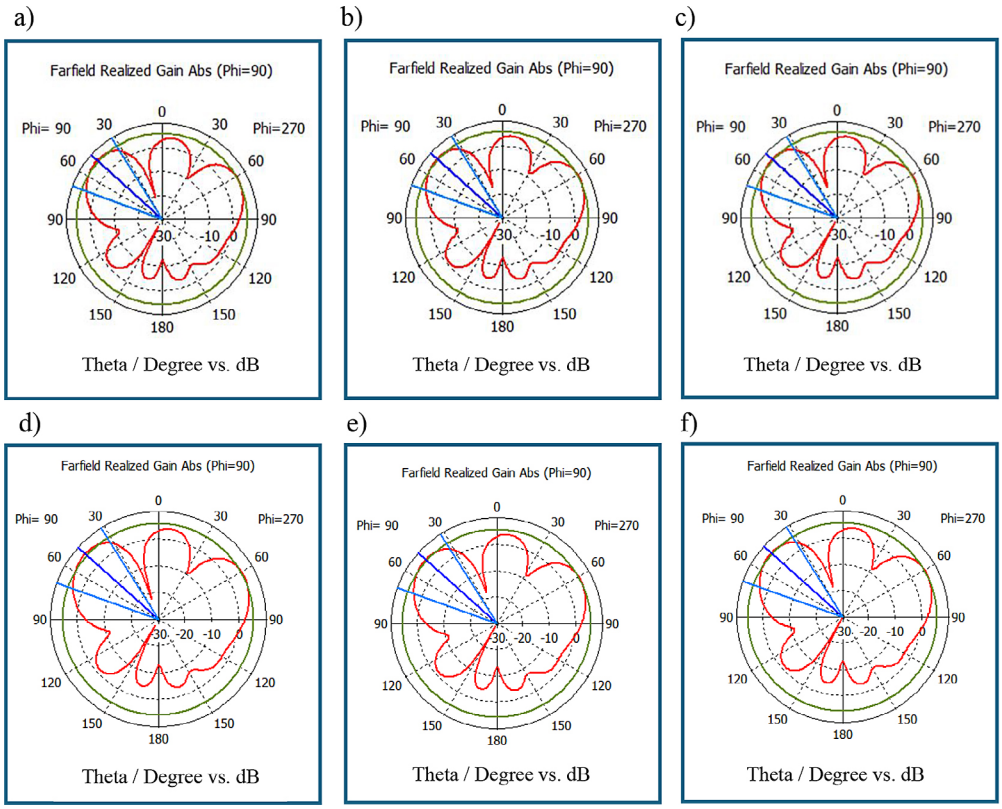

Figure 7. Radiation patterns for H (y-z) plane for copper and tantalum patch across different thicknesses: (a) 35 µm copper patch, (b) 1 µm copper patch, (c) 700 nm copper patch, (d) 35 µm tantalum patch, (e) 1 µm tantalum patch, (f) 700 nm tantalum patch

in the E-plane. Additionally, the radiation pattern in the H- plane reveals that the ET-shaped slot with parasitic rectangular patches influences the patterns in the backward direction for all antennas. The antenna's radiation pattern is directional, featuring a narrow beamwidth, which can be advantageous for certain applications requiring focused signal transmission. The appearance of back lobes in the radiation pattern can be attributed to the effects of the finite ground plane, where the ground plane slots function as resonators in the high frequency range. Table 2 summarizes the radiation characteristics and performance parameters for copper and tantalum patches at thicknesses of 35 µm, 1 µm, and 700 nm.

ANTENNA DESIGN COMPARISON WITH SOME DESIGNS FROM THE LITERATURE

Table 3 presents a comparative analysis of the proposed antennas against several recently published designs, evaluating key parameters such as substrate material, patch shape, patch material, operating frequency, reflection coefficient, S_{11}, VSWR, bandwidth, and gain.

Except for the copper 35 µm design, all proposed antennas precisely achieve the target 28.00 GHz operating frequency, making them more suitable for 5G mmWave applications than alternatives like [20], which exhibits frequency deviations of 27.01 GHz, 26.81 GHz, and 26.79 GHz. While these deviations may seem minor, they indicate a lack of precise tuning, which is crucial for stable 5G deployment. In contrast, our proposed antennas maintain a tight frequency tolerance ranging from 28.00 GHz to 28.02 GHz, ensuring better compatibility with 5G networks.

In terms of S_{11} performance, the proposed designs achieve an outstanding range from -21.145 dB to -27.391 dB, significantly outperforming the -17.17 dB reported in [21]. The lowest S_{11} in our work, -27.391 dB, is superior to the best S_{11} of -23.53 dB in [21] and -24.09 dB in [20]. A lower S_{11} value signifies better impedance matching and reduced signal reflection, ensuring higher transmission efficiency. Compared to [16], which reports S_{11} values of -45.21 dB and -39.60 dB, our work does not reach the extreme S_{11} levels but achieves a well-balanced trade-off between bandwidth and impedance matching, making it more suitable for practical 5G mmWave applications.

The VSWR values of the proposed antennas range between 1.09 and 1.19, closely aligned with the theoretical ideal of 1.00. Comparatively, [20] reports a VSWR range of 1.002 to 1.13, and [21] does not provide VSWR values. The lower VSWR values in our work indicate better impedance matching than those in [20] and ensure efficient signal transmission with minimal reflection losses.

The proposed designs maintain bandwidth values between 0.754 GHz and 0.807 GHz, ensuring sufficient bandwidth without excessive widening that could degrade signal efficiency. In contrast, [20] reports higher bandwidth values of 4.56 GHz, 4.78 GHz, and 4.49 GHz, which, although beneficial for broader coverage, introduce a trade-off in frequency accuracy. Compared to [16] which reports 1.84 GHz and 9.00 GHz, and [21] which does not provide applicable bandwidth values, our work achieves a balanced bandwidth suitable for mmWave applications.

A key distinction in this work lies in the substrate selection, patch shape, and material choices. While [16] and [21] utilize FR-4 or unspecified substrates, this work employs borosilicate glass, a material known for its low dielectric loss and superior thermal stability. This choice enhances signal transmission efficiency, reducing dielectric losses that conventional substrates suffer from.

Table 2. Performance comparison of copper and tantalum patches across three thicknesses for the proposed antennas

Ground and material	Copper			Tantalum		
Patch and ground thicknesses, (m_t)	35 mm	1 µm	700 nm	35 mm	1 µm	700 nm
Antenna parameters, (mm)						
Frequency, f_o (GHz)	28.02	28.00	28.00	28.00	28.00	28.00
Reflection coefficient, S_{11} (dB)	- 27.39	- 22.97	- 22.95	- 25.49	- 21.47	- 21.14
Voltage standing wave ratio (VSWR)	1.09	1.15	1.15	1.11	1.18	1.19
Bandwidth (GHz)	0.788	0.754	0.755	0.807	0.774	0.772
Gain (dB)	6.54	6.38	6.39	6.33	6.14	6.11

Table 3. Performance comparison of the proposed antenna with existing patch designs and materials

Paper	Substrate	Patch shape	Patch material	Patch dimensions (mm)	Frequency (GHz)	S_{11} (dB)	VSWR	Bandwidth (GHz)	Gain (dB)
[16]	Not applicable	Rectangular with two rectangular slots (semicircular at both the ends)	Copper	6.34 × 4.00	28 46	-45.21 -39.60	1.011 1.021	1.84 9.00	6.25 5.84
[20]	Rogers RT 5880	Rectangular	Gold Silver Copper	4.5 × 3.4	27.01 26.81 26.79	- 58.7 - 28.79 - 24.09	1.002 1.075 1.13	4.56 4.78 4.49	7.168 7.04 7.156
[21]	FR-4	Rectangular	Copper Aluminum Gold Silver Iron Platinum Tantalum Molybdenum	3.29 × 2.44	28.00 27.99 28.00 28.00 27.94 27.94 27.92 27.97	-17.28 -18.06 -17.63 -17.17 -21.84 -22.26 -23.53 -19.49	Not applicable	Not applicable	Not applicable
This work	Borosilicate glass	ET-shaped and three parasitic rectangular patches	Copper 35 µm Copper 1 µm Copper 700 nm	5.85 × 9.85	28.02 28.00 28.00	-27.391 -22.974 -22.954	1.09 1.15 1.15	0.788 0.754 0.755	6.54 6.38 6.39
			Tantalum 35 µm Tantalum 1 µm Tantalum 700 nm		28.00 28.00 28.00	-25.499 -21.474 -21.145	1.11 1.18 1.19	0.807 0.774 0.772	6.33 6.14 6.11

Additionally, the ET-shaped patch with three parasitic rectangular patches improves impedance matching, which is absent in the purely rectangular designs used in [20] and [21].

Another significant advantage is the optimized patch dimensions and material layering. Unlike [16] and [21], which rely on conventional rectangular patches, the ET-shaped design with three parasitic rectangular patches in this work enhances radiation efficiency and bandwidth stability. Our thinner copper and tantalum layers, ranging from 700 nm to 35 µm, allow greater flexibility in impedance optimization, reducing reflection coefficients and signal loss. In contrast, the materials used in [20] and [21] such as silver, platinum, and molybdenum, lead to greater dielectric and conductor losses, limiting their efficiency in high frequency 5G environments.

Although [20] achieves higher gain, its frequency deviation makes it less reliable for precise 5G mmWave implementation. By achieving precise frequency stability while maintaining sufficient gain, minimal signal reflection, and optimized bandwidth, this work presents a well-rounded solution for next-generation wireless applications. Optimized material selection, patch geometry, and impedance matching collectively contribute to the superior performance of this design, surpassing existing alternatives in frequency accuracy, minimal signal loss, and overall efficiency.

CONCLUSIONS

In conclusion, while copper remains the standard patch for microstrip patch antennas due to its affordability and reliability, this study demonstrates tantalum's potential as a promising alternative, particularly when fabricated using MEMS technology. The 1 µm tantalum patch demonstrated excellent performance, with an S_{11} of -21.474 dB, a VSWR of 1.18, and a gain of 6.14 dB at 28 GHz, underscoring its suitability for 5G mmWave applications. Tantalum's thin profile enables high performance and ease of fabrication, making it practical for mass production. This study highlights the critical role of patch thickness, with the 1 µm design striking an optimal balance between efficiency and manufacturability. These findings validate the proposed design and highlight tantalum's potential for advancing next-generation MEMS-based MPAs. Future research should focus on experimental validation and exploring alternative materials to enhance scalability and performance for real-world 5G systems.

Acknowledgements

This work is funded by the Ministry of Higher Education, Malaysia under the Fundamental Research Grant Scheme (FRGS) with code FRGS/1/2024/TK07/UKM/02/9, PAME SDN BHD Industry Grant (RR-2022-001), and UNITEN BOLD Grant (J510050976).

REFERENCES

1. Gnanathickam J, Thanusha G, Moses N, editors. Design and Development of Microstrip Patch Antenna for 5G Application. 2023 International Conference on Computer Communication and Informatics (ICCCI); 2023: IEEE.
2. Ma L, Liu Y, Zhang X, Ye Y, Yin G, Johnson BA. Deep learning in remote sensing applications: A meta-analysis and review. ISPRS journal of photogrammetry and remote sensing. 2019; 152: 166–77.
3. Yin J, Wu Q, Yu C, Wang H, Hong W. Broadband symmetrical E-shaped patch antenna with multimode resonance for 5G millimeter-wave applications. IEEE Transactions on Antennas and Propagation. 2019; 67(7): 4474–83.
4. Faseehuddin M, Sampe J, Shireen S, Md Ali SH. Minimum component all pass filters using a new versatile active element. Journal of Circuits, Systems and Computers. 2020; 29(5): 2050078.
5. Sciuto, G. L., Bijak, J., Kowalik, Z., Szczygieł, M., Trawiński, T. (2024). Displacement and magnetic induction measurements of energy harvester system based on magnetic spring integrated in the electromagnetic vibration generator. Journal of Vibration Engineering & Technologies, 12(3), 3305–3320.
6. Covaci C, Gontean A. Piezoelectric energy harvesting solutions: A review. Sensors. 2020; 20(12): 3512.
7. Sciuto, G. L., Bijak, J., Kowalik, Z., Kowol, P., Brociek, R., Capizzi, G. (2024). Deep learning model for magnetic flux density prediction in magnetic spring on the vibration ASTRJ-04419-2025-01 generator. IEEE Access
8. Lo Sciuto, G. Air pollution effects on the intensity of received signal in 3G/4G mobile terminal. International Journal of Energy and Environmental Engineering, 2019; 10(2): 221–229.
9. Iannacci J. Microsystem based Energy Harvesting (EH-MEMS): Powering pervasivity of the Internet of Things (IoT)–A review with focus on mechanical vibrations. Journal of King Saud University-Science. 2019; 31(1): 66–74.
10. Yahya Alkhalaf H, Yazed Ahmad M, Ramiah H. Self-sustainable biomedical devices powered by RF energy: A review. Sensors. 2022; 22(17): 6371.
11. Mohd Yunus NH, Sampe J, Yunas J, Pawi A, Rhazali ZA. MEMS based antenna of energy harvester for wireless sensor node. Microsystem technologies. 2020; 26: 2785–92.
12. Kishore S, Rajak AA. Microstrip patch antenna with C slot for 5G communication at 30 GHz. Emerging Science Journal. 2022; 6(6): 1315–27.
13. Khalid A, Sampe J, Majlis BY, Mohamed MA, Chikuba T, Iwasaki T, et al., editors. Towards high performance graphene nanoribbon transistors (GNR--FETs). 2015 IEEE regional symposium on micro and nanoelectronics (RSM); 2015: IEEE.
14. Yunus NHM, Sampe J, Yunas J, Pawi A, editors. Parameter design of microstrip patch antenna operating at dual microwave-band for RF energy harvester application. 2017 IEEE regional symposium on micro and nanoelectronics (RSM); 2017: IEEE.
15. Bakshi G, Yaduvanshi R, Vaish A, editors. Dual Band Sapphire Stacked RDR Aperture Coupled Antenna with Linear Polarization and Circular Polarization for C-Band Applications. 2019 Third International Conference on Inventive Systems and Control (ICISC); 2019: IEEE.
16. Nayak A, Dutta S, Mandal S. Design of dual band microstrip patch antenna for 5G communication operating at 28 GHz and 46 GHz. International Journal of Wireless and Microwave Technologies. 2023; 13(2): 43–52.
17. Kiani N, Hamedani FT, Rezaei P. Reconfigurable graphene-gold-based microstrip patch antenna: RHCP to LHCP. Micro and Nanostructures. 2023; 175: 207509.
18. Ramli MR, Ibrahim S, Ahmad Z, Abidin ISZ, Ain MF. Stretchable conductive ink based on polysiloxane–silver composite and its application as a frequency reconfigurable patch antenna for wearable electronics. ACS applied materials & interfaces. 2019; 11(31): 28033–42.
19. Tamayo-Dominguez A, Fernandez-Gonzalez J-M, Castaner MS. Low-cost millimeter-wave antenna with simultaneous sum and difference patterns for 5G point-to-point communications. IEEE Communications Magazine. 2018; 56(7): 28–34.
20. Shoaib HM, Snigdho MK, Islam AKME, editors. Comparative Study on the Performance of Microstrip Patch Antenna using Gold, Silver, and Copper as Radiating Surfaces. 2024 Second International Conference on Emerging Trends in Information Technology and Engineering (ICETITE); 2024; 22–23 Feb. 2024.
21. Hiçdurmaz B, Gümüş ÖF. Design and analysis of 28 GHz microstrip patch antenna for different type FR4 claddings. Uludağ Üniversitesi Mühendislik Fakültesi Dergisi. 2019; 24(2): 265–88.
22. Redzuwan RM, Sampe J, Latif R, Rhazali ZA, Yunus NHM. Design of a High-Gain MEMS-Based Microstrip Patch Antenna for RF Energy Harvesting in Millimeter-Wave 5G Applications. SSRG International Journal of Electrical and Electronics Engineering. 2024; 11(9): 316–25.